

W. Cheng · P. B. Rhines

Response of the overturning circulation to high-latitude fresh-water perturbations in the North Atlantic

Received: 26 March 2003 / Accepted: 20 November 2003 / Published online: 27 February 2004
© Springer-Verlag 2004

Abstract Studies have suggested that sea-ice cover east and west of Greenland fluctuates out-of-phase as a part of the Atlantic decadal climate variability, and greater changes are possible under global warming conditions. In this study, the response of the Atlantic meridional overturning circulation (MOC) to the distribution of surface fresh-water flux is explored using a global isopycnal ocean model. An Arctic ice related fresh-water flux of 0.1 Sv entering the Nordic Seas is shown to reduce the maximum overturning by 1 to 2 Sv ($10^6 \text{ m}^3 \text{ s}^{-1}$). A further decrease of 3 to 5 Sv in the MOC is observed when the fresh-water flux is shifted from the Fram Strait to the southern Baffin Bay area. Surprisingly, the salinity in much of the upper Nordic Seas actually increases when the Arctic fresh-water source is the strongest there, as a result of enhanced global overturning. It reflects the great influence of Labrador Sea convection on this model's MOC. By applying a weaker surface fresh-water transport perturbation (0.02 Sv) on the Baffin Bay area and therefore perturbing the Labrador Sea Water (LSW) formation, we have also investigated the interaction between the overflows across the Greenland–Scotland Ridge and the LSW and find that, with the same surface forcing conditions in the Nordic Seas, volume transport of the overflows weakens when the LSW formation intensifies.

1 Introduction

A dominant mode of low-frequency climate variability in the Atlantic, the North Atlantic Oscillation or the Northern Annular Mode (Thompson and Wallace 2000), has regional as well as global expressions (Hurrell 1995;

Dickson et al. 2000; Delworth and Dixon 2000). A recent study using buoy ice-motion data has shown that during high NAO phase, Arctic ice export through the Fram Strait tends to increase (Rigor et al. 2002). This result is in agreement with satellite observations (Kwok and Rothrock 1999) and numerical simulations (Zhang et al. 2000). It has also been suggested that ice cover bordering the Labrador Sea has fluctuation out-of-phase with that in the Greenland Sea on interannual and longer time scales. The latter shows a persistent decrease from the late 1960s (Dickson et al. 1996; Deser et al. 2000) until the recent years, coincident with the time when the NAO is moving toward its large positive index state which one expects to cause increased ice melting in the Greenland Sea.

A key element in the climate response to increasing greenhouse gases is the likely increase in fresh-water loading of the Arctic and subpolar Atlantic oceans. These scenarios also suggest the possibility that fresh-water transport from the Arctic into the North Atlantic can shift between passages on either side of the Greenland. The complexity and small scale of the pathways connecting the Arctic and the North Atlantic challenge climate models, which typically have coarse resolution. While current climate models are not able to resolve all of these satisfactorily, investigation of climate response to fresh-water sources needs to be pursued in detail. In particular, it is important to examine the contributions from the Labrador Sea Water (LSW) and overflows across the Greenland–Scotland Ridge on the global meridional overturning circulation (MOC) as they appear in these models.

Previous studies on the response of the MOC to changes in high-latitude fresh-water flux often apply perturbations evenly along the latitude circle (e.g., Manabe and Stouffer 1995). In reality, the Great Salinity Anomaly (GSA) episodes (Belkin et al. 1998) start as regional signals which later propagate around the sub-polar gyre. During its transit, the influence of a GSA on the multiple downward transport branches of the MOC may vary.

W. Cheng (✉) · P. B. Rhines
School of Oceanography, University of Washington,
Campus Box 355351, Seattle, WA 98195, USA
E-mail: wcheng@ocean.washington.edu

The overall goal of this study is to better understand the relationship between deep water production and the MOC in the North Atlantic. In particular, we want to investigate which of the following deep water components, the overflows or the LSW, dominate the MOC. Furthermore, are there feedbacks between these deep water branches when either of them is perturbed? Finally, what is the impact of a 15–20% reduction of the MOC that are typical of multi-decadal variability of the MOC, as compared to a complete shut down of the thermohaline circulation, on the global temperature and salinity distributions, especially those in the Arctic? These are some crucial, yet largely unanswered, questions regarding high-latitude climate and its variability.

We employ the layered Miami Isopycnal Coordinate Ocean Model (MICOM) in the study. Layer models like MICOM have the potential to give a more accurate representation of the deep circulation by preserving water masses as they descend to great depth. We ran four numerical experiments (summarized in Table 1). In the “control” experiment, the model is driven by monthly climatology of the surface atmospheric conditions. In the “Fram” experiment, besides the climatological surface forcing, 0.1 Sv of surface fresh-water flux is extracted from the Arctic and distributed across the Fram Strait to mimic the ice flux induced fresh-water transport. The “Baffin” experiment is otherwise the same as the “Fram” experiment, except now that the 0.1 Sv fresh-water transport takes place across the Baffin Bay area. Finally, the “Baffin-weak” experiment repeats the “Baffin” experiment, except with a much weaker fresh-water transport perturbation (0.02 Sv instead of 0.1 Sv). This experiment design means that the globally averaged surface fresh-water flux is the same in all model runs, but its spatial distribution is different from one run to the other. The underlying idea is twofold. Firstly, we want to investigate whether the MOC is sensitive to zonal redistribution of a constant fresh-water load in the sub-polar North Atlantic. Secondly, the fresh-water transport perturbations were located directly upstream of the primary North Atlantic deep water formation sites. The intention was to perturb the individual deep waters one by one and to study the interaction between them. The fresh-water transport of 0.1 Sv is equivalent to the observed long-term mean ice flux through the Fram Strait, which is at an amplitude of approximately 3000 km³/year (Kwok and Rothrock 1999). To facilitate an easy comparison between the Fram and Baffin experiments, we used the same amount of fresh-water transport per-

turbation in both runs. The fact that the mean ice flux through the Davis Strait is smaller than that through the Fram Strait (336 km³/year for the former) is latter addressed by the Baffin-weak experiment.

The study is organized as follows. In Sect. 2, we describe the MICOM model and the surface forcing conditions used to drive the model; in Sect. 3 the sensitivity of the MOC to the surface fresh-water transport perturbation is studied and processes responsible for such sensitivity are identified; major conclusions from this study are summarized in Sect. 4, in addition to a brief discussion on their climatic implications.

2 The model and surface forcing conditions

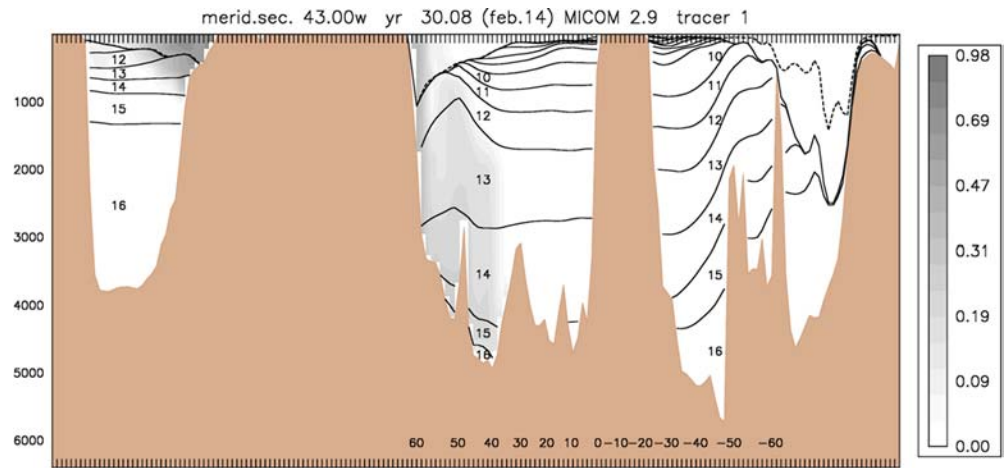
Detailed description of the Miami Isopycnal Coordinate Ocean Model (MICOM) can be found in Bleck and Boudra (1986), Bleck et al. (1989). To use the model on global domain and to avoid the North Pole singularity associated with Mercator projection, a special grid orientation called bipolar projection (Arfken 1970, ch 2.9) is used north of 57°N. An advantage of the bipolar projection is that it merges smoothly with the Mercator projection at the transition latitude where the two meet. As such, a continuous and consistent transport of water mass and its properties is maintained at the transition latitude. Since the northernmost model grid point starts at the Bering Strait, transport through this strait is prescribed to be 1.0 Sv. The thermodynamic sea-ice model we developed is a simple energy balance calculation in which the amount of ice formed in winter at each grid point is determined by the latent heat release needed to keep the mixed layer (ML) temperature from dropping below freezing point. Energy thus lent to the ocean is repaid in summer when surface heat input to the ocean must melt the ice before warming the ML. The rest of ice thermodynamics, namely, the heat balance at the upper and lower interfaces of the ice and the energy transfer within the column, follows the “0-layer” model of Semtner (1976). Ice dynamics is neglected.

Essentially, MICOM describes the interior of the ocean as a stack of layers, each with fixed potential density and interacting with others primarily through pressure gradient force. The ML and fossil ML (see explanation later) atop the isopycnals provide the link between the external forcing and the interior ocean. For an isopycnal layer, besides the governing shallow water equations, a conservation equation for salt is used to predict the salinity while the temperature is diagnosed from salinity and potential density using a polynomial seawater state equation. Separate heat and salt balance calculations are carried out only in the MLs according to the Kraus-Turner scheme (Kraus and Turner 1967), which, also predicts the ML thickness according to the turbulent kinetic energy conservation equation. Diapycnal mixing in the model is handled by the MacDougall and Dewar (1998) scheme which solves a diffusion equation for layer temperature, salinity and layer thickness while keeping the density, in each layer, constant. Due to the more realistically simulated lateral advection and diapycnal mixing, isopycnal models are believed to have a better representation of water mass structure and the tilting and packing of isopycnals associated with strong baroclinicity of the ocean. Figure 1 shows a meridional cross section of the model with the Arctic on the leftmost side (notice that due to the Mercator Projection used, the latitude ticks are not equally spaced). It shows the well preserved subtropical fronts in both hemispheres; the tilting of isopycnals around 50°S that are associated with the Antarctic Circumpolar Current (ACC); doming of the isopycnal at 55°N during this time period which is consistent with observations, and the deep ML at the northern high latitudes. Leaning of the isopycnals against bottom topography at 50°N implies a bottom current associated with the Denmark Strait Overflow coming from the east. A tracer released in the surface Nordic Seas is also shown in this section. More discussions on the tracer distribution will be presented later.

Table 1 Summary of experiments

Experiment	Fram Strait FW transport anomaly	Baffin Bay FW transport anomaly
Control	0.0 Sv	0.0 Sv
Fram	0.1 Sv	0.0 Sv
Baffin	0.0 Sv	0.1 Sv
Baffin-weak	0.0 Sv	0.02 Sv

Fig. 1 Snapshot of a vertical section along 43°W in the model. *Solid lines* represent layer interface and the *dashed line* represents the base of the ML. Layer number is marked if space permits. *Shading* represents concentration of a tracer injected steadily at the surface of the Greenland Sea



The model has a total of 16 vertical layers. The prescribed potential density (σ_2) values for layers 3 through 16 can be found in Fig. 9. The horizontal resolution is $2^\circ \times 2^\circ \cos(\phi)$ where ϕ is the latitude. The bottom topography in the model is realistic given the horizontal resolution, i.e., no further smoothing or approximation is used except that the ocean depth at any grid point is assumed to be no shallower than 100 m. Because of no smoothing of the topography, except the shallow and narrow continental shelves, most of the important topographic features of the global ocean are well preserved in the model, including, to list a few examples, the deep basins in the central Arctic and the Greenland and Norwegian seas, the marginal seas around the rim of the Arctic, and the shallow sill across the Denmark Strait and Iceland–Scotland Ridge (on the order of 500 m) (Fig. 2). The Canadian Arctic Archipelago (CAA) passage is captured to some extent by the model, which opens to the slightly deeper Baffin Bay.

We also incorporated a second non-isopycnal layer, a “fossil ML”, to improve the model representation of surface stratification in the Arctic. In earlier experiments with a single ML, when the detrained ML water (with arbitrary density values) could not be

accommodated by any of the interior isopycnals (with fixed density) and was forced to stay in the ML, the ML thickness bias led to an underestimation of the warming and freshening of the surface layer during the restratification season, which, eventually destroyed the shallow Arctic pycnocline. An intermediate layer allowing horizontal density distribution accepts the detrained old ML water (thus the word “fossil”) freely and helps to maintain the stratification. To maintain its own mass balance, the fossil ML exchanges mass and water properties with the interior isopycnals following the ML detrainment algorithm used in MICOM (Bleck et al. 1989).

The model was initiated from a motionless state and Levitus (1994) annual mean layer thickness, temperature and salinity profiles. Surface forcing data were obtained from the Ocean Modeling Intercomparison Project (OMIP) web site at the Max Planck Institute for Meteorology. It includes monthly climatologies of surface wind stress, 10 m wind speed, 2 m air temperature and specific humidity, precipitation, and net radiation flux based on the ECMWF reanalysis. Air-sea sensible and latent heat (hence evaporation) fluxes are calculated using modeled ML temperature and given atmospheric states through the bulk aerodynamic formula. The surface fresh-water flux is translated to salinity flux by $S_f = (E - P - R) * 35.0$ where S_f is the surface salinity flux, and E , P , R is evaporation, precipitation and river runoff (Perry et al. 1996), respectively. Newly formed ice is assumed to have a mean salinity of 10.0 psu. All integrations have been carried out for 50 years.

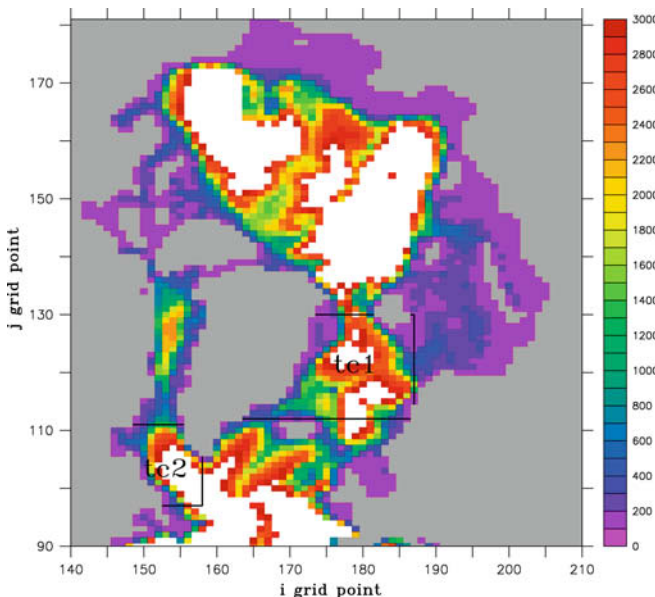


Fig. 2 Model bottom topography in the Arctic and northern North Atlantic. *White areas* indicate basins deeper than 3000 m. The *boxes* show where the ML tracers (termed ‘tc1’ and ‘tc2’, respectively) are released

3 Results

3.1 The MOC index

The time series of the maximum annual mean meridional mass transport stream function in the Atlantic, hereafter referred to as the MOC index, shows that the MOC in all simulations has reached a quasi-equilibrium state about two decades after the initialization (Fig. 3, results presented hereafter will be from year 20 to 50 if not specified otherwise). There is a minor downward trend in the MOC index in the Fram and Baffin-weak experiments near the end of the simulation, which are caused by remaining adjustment in the deep ocean. Overall, the applied fresh-water transport anomaly has a significant impact on the MOC in the model. For example, the MOC index in the Fram experiment (when the fresh-water anomaly is exported into the Nordic Seas at a rate of 0.1 Sv) shows a systematic weakening

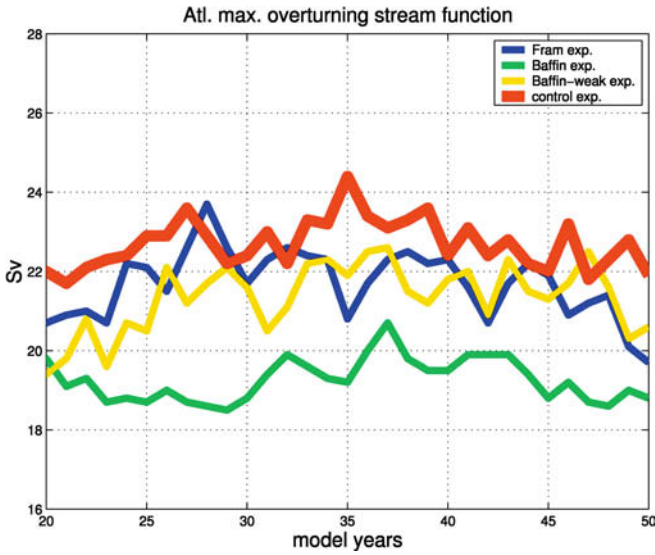


Fig. 3 Time series of the maximum annual mean meridional volume transport stream functions in the Atlantic Ocean

comparing to that in the control experiment: the mean MOC in the control run was 23 Sv, and is reduced to 21 Sv in the Fram experiment. The MOC is further decreased by 3 to 5 Sv when the fresh-water anomaly is exported to the southern Baffin Bay and Davis Strait instead of the Fram Strait. When subjected to a weaker perturbation of fresh-water flux, the MOC in the Baffin-weak experiment is of similar magnitude to that in the Fram experiment. These results suggest that a constant fresh-water transport perturbation has a larger effect on the MOC when it reaches the North Atlantic through the passage west of Greenland. This fresh-water transport anomaly directly influences LSW formation as will be shown. Superimposed on the quasi-steady states of the MOC in all simulations are interannual to longer time scale fluctuations, but their amplitudes appear to be small (1 std of the MOC index in the Control, Fram, Baffin, and Baffin-weak experiments is 0.6 Sv, 0.9 Sv,

0.6 Sv, and 0.8 Sv respectively). In this study we are interested on the processes which control the mean states of the MOC in the simulations and will leave the subject of interannual variability for future work.

3.2 The overflows and the Labrador Sea water

The relative contributions of the deep water formed north and south of the Greenland–Scotland Ridge to the North Atlantic Deep Water (NADW) production have been investigated in observational (Washington 1976; McCartney and Talley 1984; Dickson and Brown 1994; Schmitz 1995) and numerical studies (Speer and Tziperman 1992; Döscher and Redler 1997). To address this question using our simulations, it is necessary to investigate whether the coarse resolution model is able to resolve adequately the distinct water masses, in particular, the Denmark Strait Overflow Water (DSOW) and the overflow through the Iceland–Scotland Ridge, and their circulation structures. This has been a challenging problem for Cartesian-coordinate models in part because of the spurious diapycnal mixing caused by the horizontal advection schemes used in these models (Griffies et al. 2000). An isopycnal model may pose less of a problem in this regard. To investigate if it is true, multi-year mean volume transports through the Davis Strait, the Denmark Strait, and the Iceland–Scotland Ridge (location of the vertical sections are marked on Fig. 4) are calculated and compared with nearby available observations. To distinguish the surface “inflow” into the Arctic (with a positive transport) from the deep “outflow” to the North Atlantic (negative transport), the total transport is divided into the “upper” and “lower” components, separated by the upper interface of layer 13. The rationale behind this division is that the prescribed density value for layer 13 ($\sigma_2 = 36.95$) corresponds closely to the observed LSW density characteristics. It appears that the transports across all these sections in the model are highly sensitive to the location

Fig. 4 Vertical sections through which volume transport across the Davis Strait, Denmark Strait, and Iceland–Scotland Ridge is calculated (results are summarized in Table 2). Local topography is shown shaded as a reference

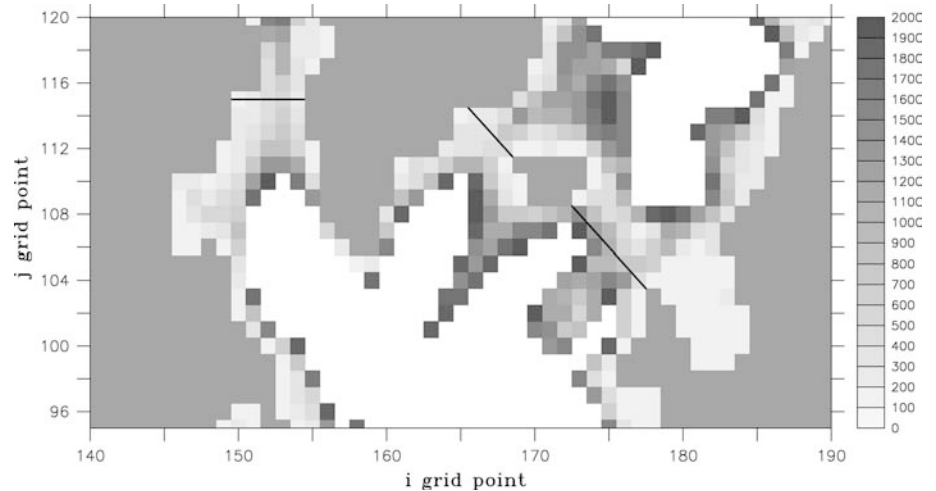


Table 2 Net volume transport across the sections marked on Fig. 4. Plain numbers refer to the Fram experiment, numbers in parentheses are from the Baffin experiment, and those in square parentheses are from nearby observations if they are available

	Davis Strait	Denmark Strait	Iceland–Scotland Ridge
	F (B) [O]	F (B) [O]	F (B) [O]
Upper (Sv)	0.0 (–1.0)	–0.7 (0.6) [–0.7 ± 0.8]	7.1 (6.1) [6.8 ± 0.5, 8.0]
Lower (Sv)	–4.4 (–1.5)	–1.7 (–2.4) [–2.7 ± 0.7]	–1.3 (–2.8) [–1.0 ~ –1.5, –2.0, –2.3 ± 1.9]
Total (Sv)	–4.4 (–2.5) [–1.2, –2.0]	–2.4 (–1.8)	5.8 (3.3)

of the fresh-water transport perturbations. For example, the outflow at the Denmark Strait decreased from –2.4 Sv in the Baffin experiment to –1.7 Sv in the Fram experiment, which is consistent with the fact that surface water in the overflow formation region is freshened in the Fram experiment. In contrast, the transport of water through the upper layers at the same section is southward in the Fram experiment (–0.7 Sv) but northward (0.6 Sv) in the Baffin experiment. In general, these numbers are in reasonable agreement with direct measurements and/or inverse model results (see Table 2 for a summary). Both direct measurements (Dickson et al. 1996; Girton and Sanford 2001) and inverse modeling (Mauritzen 1996) suggest that the transport of water denser than $\sigma_0 = 27.8$ through the Denmark Strait is on the order of -2.7 ± 0.7 Sv, while according to inverse modeling, transport at the same channel through the shallower layers is -0.7 ± 0.8 Sv. Based on the inverse method, Mauritzen (1996) proposed a formation scheme for the overflow waters in which property of the North Atlantic inflow change gradually as it enters the Norwegian Sea and circulates around the Arctic, eventually returns to the North Atlantic as boundary currents. This scheme minimizes the role of deep convection in the interior of the Nordic Seas on the formation of the overflows. It suggests an inflow of 6.8 ± 0.5 Sv warm and salty North Atlantic water enters the Nordic Seas between Iceland and Scotland, and after water mass transformation, -2.7 ± 0.7 Sv returns to the Atlantic through the Denmark Strait and -2.3 ± 1.9 Sv through the Iceland–Scotland Ridge, among the latter -1.0 ± 0.7 Sv is through the Faroe Bank Channel. ADCP data suggests that transport of water colder than 0.3°C through the Faroe Bank Channel varies between –1.0 Sv and –1.5 Sv interannually (Hansen et al. 2001). By comparison, our model simulated lower-level transport across the Iceland–Scotland Ridge is –1.3 Sv in the Fram experiment and –2.8 Sv in the Baffin experiment, both are within the range suggested by observations. On the vertical structure of the transport through the Iceland–Scotland Ridge, an early observational estimate suggests that the northward inflow is +8.0 Sv (McCartney and Talley 1984) while the outflow is –2.0 Sv. The corresponding model inflow(outflow) is +7.1 Sv(–1.3 Sv) in the Fram experiment and +6.1 Sv(–2.8 Sv) in the Baffin experiment.

To track the overflow waters as they go over the ridges and so to understand how they contribute to the NADW formation, we simulated passive tracers into the modeled mass transport field. The “off-line” simulation utilizes

the archived three dimensional mass fluxes and layer thickness distribution, and integrates the the continuity equation in the model while neglecting other model equations, in other words, the monthly-mean mass fluxes are used with the advection scheme in the MICOM to transport passive tracers both isopycnally and diapycnally. The computation efficiency of the off-line method makes it possible to run multiple tracers numerous times when needed. We compared a test tracer distribution from the off-line simulation with that from the on-line calculation and found that they produce nearly identical results. The consistency not only lends credibility to the off-line method itself but also suggests that synoptic variability in the mass transport fields (which is filtered out by monthly averaging) has negligible effect on the tracer distribution in coarse resolution models.

Throughout the simulations, the tracer concentration is set to be 1.0 constantly in two places: the ML of the Greenland–Norwegian Sea north of the Denmark Strait sill (tracer is called ‘tc1’), and the ML of the Labrador Sea (tracer is called ‘tc2’). Figure 2 shows the tracer replenish domains. The simulation was started at the end of year 20 of the MICOM integration and carried forward in time for 30 years, ending when the on-line calculation ended.

As time passes by, the surface tracer released in the Greenland Sea has penetrated into the dense layers and has been transported across the sill into the subpolar North Atlantic and into the central Arctic (Fig. 5 left column). The southward transport takes place across both the Denmark Strait and the Iceland–Scotland Ridge, these branches later join the cyclonic circulation in the subpolar latitudes and merge into the Deep Western Boundary Current (DWBC). In addition to being renewed by water of overflow origin, the subpolar and midlatitude western Atlantic is also ventilated by convection in the Labrador Sea, as suggested by ‘tc2’ distributions (Fig. 5 right column). Convection in the model is embedded in the mixed layer physics (aside from convective adjustment which operates occasionally), more specifically, in the deepening of the ML. Because the diapycnal mass flux is defined as the amount of water parcel transferring across all layer interfaces, the effect of convection is represented in the diapycnal mass flux, which then drives the tracer distribution. The broadening of the zonal extent of the ‘tc2’ occupation with time is due to the recirculation emanating from the boundary current as well as diffusion. As a result, the meridional advancing speed of the southern tip of ‘tc2’ is approximately 15° latitudes per decade, which, is weaker

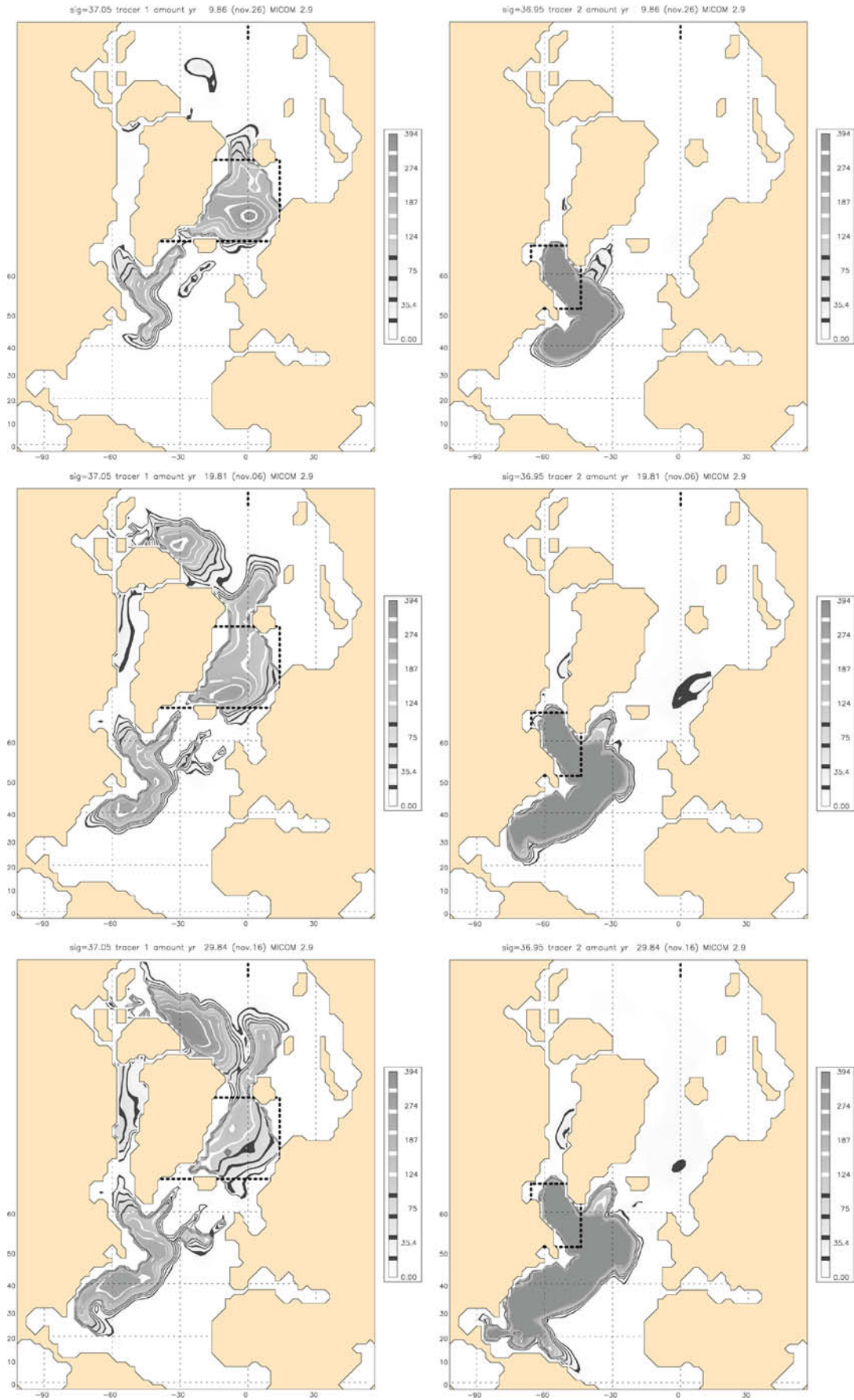




Fig. 5 Tracer inventory (concentration \times layer thickness, unit: m) in the Baffin experiment of $\sigma_2 = 37.05$ (left column, for 'tc1') and $\sigma_2 = 36.95$ (right column, for 'tc2') layers. Top to bottom frames represent $\sim 10, 20, 30$ years into the simulation. Dashed lines enclose where the ML tracers are replenished

than observed core speed of the DWBC. Tracer distribution from the Fram experiment (not shown) is similar except there the relative contributions of overflows and LSW on the Western Atlantic ventilation is changed such that the contribution from the overflows (LSW) is weakened (strengthened). Lastly, a central property of the observed ocean is the vertical separation of deep and intermediate waters (originating in the overflows east of Greenland and Labrador Sea, respectively) (McCartney 1992; Dickson et al. 1996). In the model, the globally averaged 'tc2' peaks at $\sigma_2 = 36.95$ while 'tc1' peaks at $\sigma_2 = 37.05$ (Fig. 6), the mean depth of the layer is 2500 m and 4500 m respectively. Though our model exhibits the separation to some degree, it is probably not as strong as in nature. Larger 'tc2' than 'tc1' concentration in the deepest layer towards the end of the simulation can be due to mixing process which increases LSW water mass, and overall faster ventilation rate in the Labrador Sea.

These results suggest that the model is able to reproduce some basic characters of the LSW and overflow waters. Next, we want to investigate how the two water masses may interact with each other, in particular, how the overflows would respond to a changed LSW

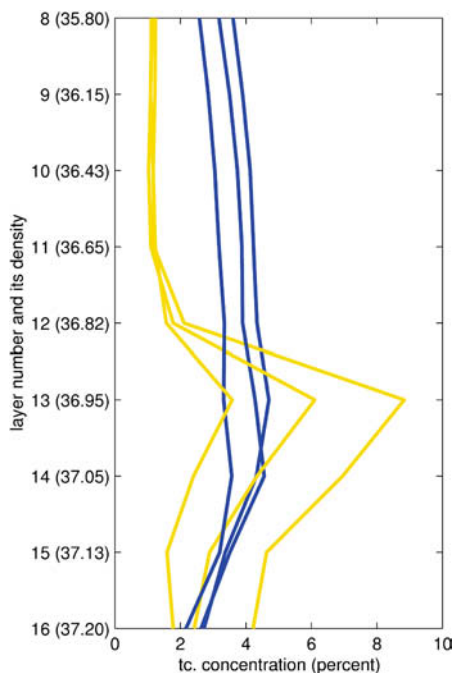


Fig. 6 Globally averaged tracer concentration as a function of layer number (only deep layers are shown). Black lines represent 'tc1' and gray lines represent 'tc2'. Lines in each color group from left to right correspond to roughly 10, 20, 30 years into the simulation

formation. Such a knowledge should help us to better understand processes controlling the overflow variability. To study this, we perturb the LSW formation by applying a weaker surface fresh-water anomaly in the Baffin Bay area (the "Baffin-weak" experiment). The weaker forcing of 0.02 Sv is comparable with the mean ice flux through the Davis Strait. The meridional volume transports across several latitudes in the North Atlantic in this case are binned against their temperature and salinity values for 0.5 °C and 0.025 psu intervals and compared with the results from the Baffin experiment (Fig. 7). Transport of the water as a function of temperature and salinity not only enables us to understand the magnitude of the circulation, it provides insight on along-path water property evolution. Interestingly, although all surface forcing conditions are the same in the "Baffin" and "Baffin-weak" experiments in the overflow formation regions, the volume transport of the overflow turns out to be quite different from one case to the other. Across 65°N which represents the shallowest sill in the Denmark Strait, southward transport of water denser than $\sigma_2 = 37.05$ (the density of the overflow) is 3.6 Sv in the Baffin experiment and decreases to 1.3 Sv in the Baffin-weak case. Meanwhile, owing to a weakened fresh-water cap in the northern Labrador Sea, southward transport of water with $T = 4.0$ °C and $S = 35.20$ psu across 50°N has intensified in the Baffin-weak experiment (Fig. 7 middle row). Interestingly, the modeled overflow transport responds strongly to the LSW formation: when the latter is stronger, the former weakens. Since this change occurs under fixed surface forcing conditions in the overflow formation region, it is likely controlled by ocean internal processes. Further downstream of the DWBC, at 35°N which is the central latitude of the maximum overturning, further freshening of the water mass (Fig. 7 bottom row) is caused by a mixing of the NADW with the Antarctic Intermediate Water reaching from the south. There the total southward transport of water denser than $\sigma_2 = 36.95$ is 20.9 Sv in the Baffin-weak experiment and 18.7 Sv in the Baffin case, suggesting that the increase of the Labrador Sea outflow in the Baffin-weak experiment have dominated the overflow weakening signal.

3.3 3-D structure of the MOC

In this subsection we study the relationship between deep water formation and the MOC, the former is a water mass transformation process which does not automatically mean overturning, as the newly formed deep water can be stagnant or transferred laterally without sinking. This difference between deep water formation and the MOC is similar to the distinction between convection (which produces dense deep water) and downwelling (Send and Marshall 1995; Marotzke and Scott 1999; Spall and Pickart 2001).

There are several ways to portray the MOC in a global ocean model. A commonly used one is the zonally

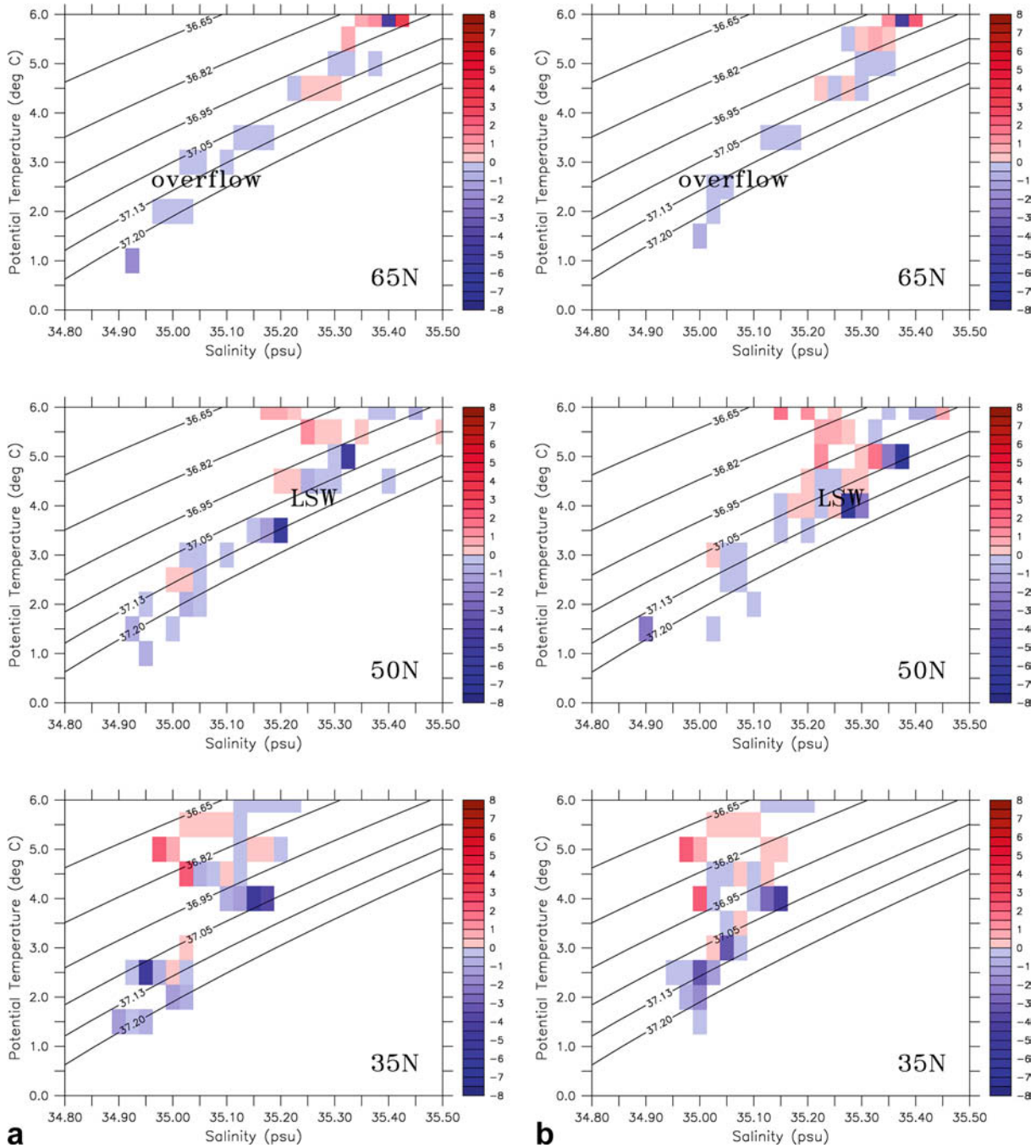


Fig. 7a, b Volume transport (units: Sv) of water colder than 6 °C across several latitudes in the North Atlantic on $\theta - S$ space. *Positive* means net northward transport. Labrador Sea water

formation is seen as *bold points* (high transports) (3–5 °C) in the *middle row*. **a** Baffin experiment; **b** Baffin-weak experiment

integrated mass transport stream function on either σ - y or z - y space (Fig. 8). Since MICOM uses potential density as its vertical coordinate, the MOC is readily available on y - σ space (Fig. 9a, b for the Baffin and Fram experiments, respectively). This presentation more naturally describes water mass transformation than does the y - z space stream function (Mauritzen and Häkkinen 1999). In both experiments, the majority of the lower level southward transport has transversed into the

Southern Hemisphere, indicating that the “Veronis Effect”, the upwelling in the midlatitude western boundary layer region (Veronis 1975), is nicely suppressed in the model. The climbing of stream lines to lighter layers near the equator is a manifestation of the wind-driven upwelling, which, as expected, is negligibly different between the two runs. The major differences between the two runs exist in the higher density class, especially in layers denser than $\sigma_2 = 36.95$. This difference cell extends

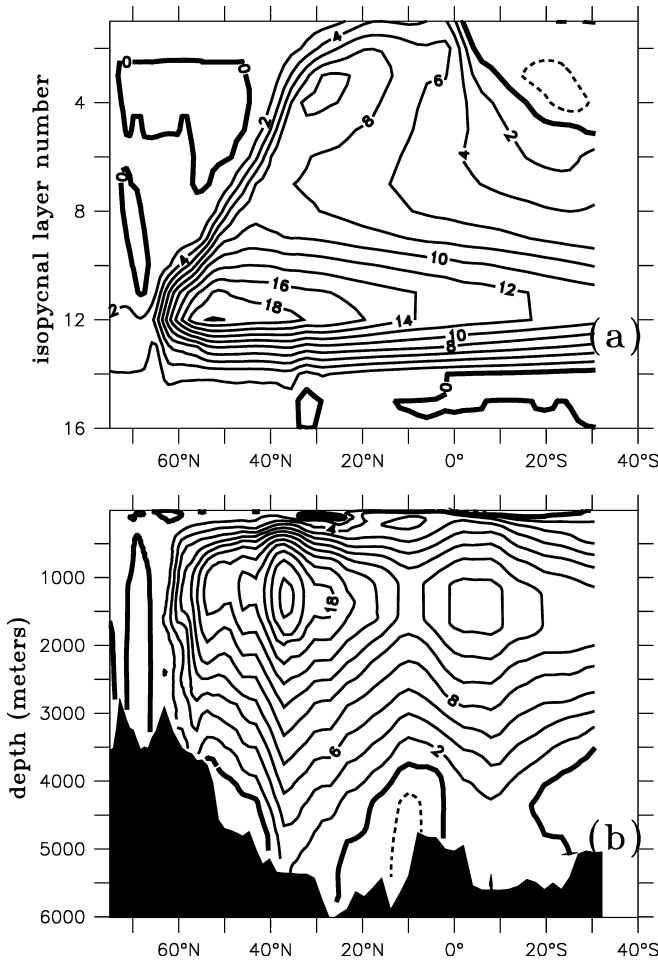


Fig. 8 An example of the meridional overturning stream function depicted in **a** σ - y space, **b** z - y space

meridionally over the entire ocean to its southern boundary (Fig. 9c), even though half of the stronger downward transport in the Fram experiment is recirculated within the North Atlantic itself. The climatic consequence of a stronger MOC in the Fram experiment is an increased meridional heat transport of 0.04 PW (1 PW = 10^{15} Watts) from the southern boundary of the Atlantic to 30°N (Fig. 9d), north of which the heat transport anomalies shows convergence. The magnitude 0.04 PW is equivalent to 5% of the maximum heat transport in the subtropics, and is of the same order as the heat transport response observed in a numerical study by opening the Canadian Archipelago (Goosse et al. 1997).

Although the zonally integrated stream function shows the overall character of the overturning circulation, it does not capture all aspects of the three-dimensional MOC. A complement to this is the horizontal transports on isopycnal surfaces. They are calculated as:

$$U = \sum_{k=k_1}^{k=k_2} u_k \Delta y h_k$$

$$V = \sum_{k=k_1}^{k=k_2} v_k \Delta x h_k$$

where (U, V) are the vertically integrated volume transports in Sverdrups, (u_k, v_k) are the along-isopycnal velocity components (units: cm/s), h_k is the layer thickness (m), and $\Delta x, \Delta y$ is the zonal and meridional grid box size respectively. Again the vertical integration is computed for the “upper” ($k_1 = 1, k_2 = 12$) and “lower” ($k_1 = 13, k_2 = 16$) density classes separately. In the Fram experiment, the upper transport of the subtropical western boundary current splits into three branches north of the Newfoundland coast (Fig. 10a). The North Atlantic Drift continues northeastward and finally into the Nordic Seas, a second branch moves northward into the Irminger Sea, and the third one turns northwestward into the Labrador Sea. A striking feature in the upper-level transport pattern is that the transport is much weaker when it reaches the western Labrador Sea than on the west coast of Greenland. For a quasi-steady ocean with negligible change in layer thickness, the horizontal mass transport should balance roughly by the vertical transport. The weakening thus implies a strong convection in the western Labrador Sea which converts a large amount of water into the dense water class. As a result, the lower layers southward transport is enhanced greatly at the subpolar latitudes (Fig. 10b). Relative to that in the Baffin experiment, the upper transport in the Fram experiment along the western Greenland coast is even larger while the transport in the western Labrador Sea is even weaker (Fig. 10c), and the cyclonic circulation in the lower layers is also strengthened (Fig. 10d). The intensified Labrador Sea convection in the Fram experiment drives an overall stronger MOC despite a weakened southward overflow across the Greenland–Scotland Ridge (Fig. 10d). Under the same fresh-water transport perturbation through the Fram or the Davis Strait, western Labrador Sea convection is weakened more in the latter case, and the strength of the basin scale MOC is dominated by LSW formation than by the overflows.

This analysis infers diapycnal mass flux from its isopycnal components. A more direct approach of understanding deep water formation is to estimate the warm-to-cold water transformation rate across a density interface (Speer and Tziperman 1992). This can be done quite straightforwardly in an isopycnal model. Again we computed the transformation across the upper interface of layer 13 ($\sigma_2 = 36.95$) for reasons stated previously. The sign convention is such that a positive value means transformation of water from a lighter to a denser layer. In the North Atlantic, a total of 20.6 Sv transformation takes place in the Fram experiment, compared to a total of 17.7 Sv in the Baffin case (Fig. 11). In terms of spatial distribution, the transformation is concentrated in the subpolar latitudes, more specifically, in the Labrador and Irminger seas, with some minor contributions from the Greenland–Norwegian Sea region. When we further

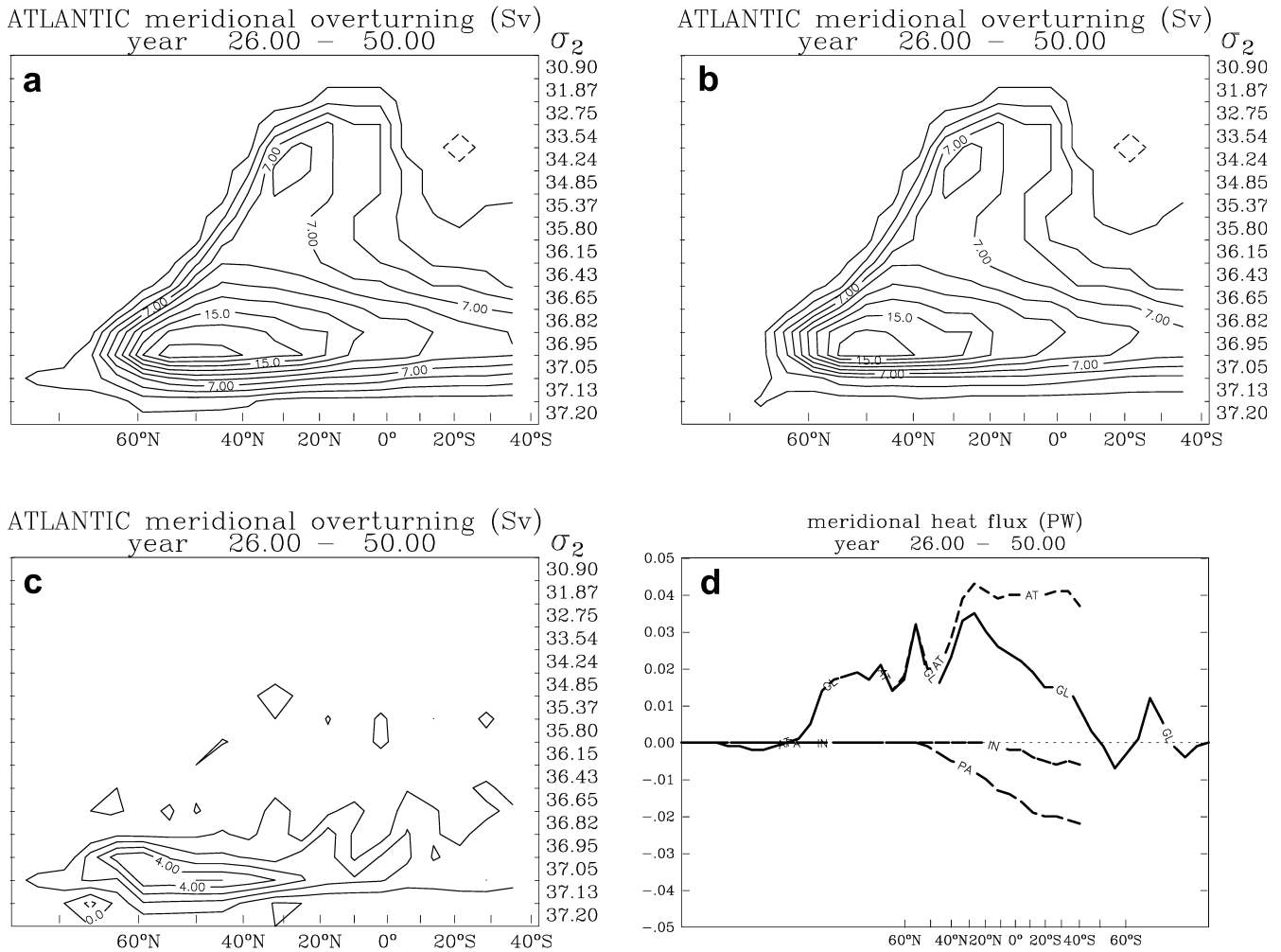


Fig. 9 Long term mean meridional overturning stream function in the Atlantic Ocean (units: Sv): **a** the Fram experiment; **b** the Baffin experiment; **c** Fram minus Baffin experiment. **d** The difference in the ocean heat transport (OHT) (Fram experiment minus Baffin

experiment). *AT*, *GL*, *IN*, and *PA* correspond to the Atlantic, global, Indian, and Pacific Ocean, respectively. The vertical coordinates in **a**, **b**, **c** are potential densities. The contour interval used in **a** and **b** is 2.0, in **c** it is 1.0

divided the northern North Atlantic into western and eastern subdomains according to the longitude of Cape Farewell, the transformation rate is 17.9 Sv and 2.7 Sv respectively in the Fram experiment and 12.4 Sv and 5.3 Sv respectively in the Baffin case. Obviously, the reduced total transformation rate in the subpolar North Atlantic in the Baffin experiment is due to the weakening of dense water formation in the western subdomain, caused by the flood of buoyant fresh-water at the surface. Changes in the eastern subdomain oppose those in the Labrador Sea but with weaker amplitudes.

It is thus apparent that the main driving force for the stronger overturning in the Fram experiment is the LSW formation. Does this mean that the corresponding global ocean temperature and salinity anomaly is also concentrated in the subpolar latitudes? The short answer to this question is no. The averaged salinity of the upper layers in the Fram experiment is saltier than that in the Baffin experiment over the northern Greenland Sea, the eastern Fram Strait and Arctic Siberian Sea, and part of

the Canadian basin (Fig. 12a). Such an extensive salinity anomaly, especially that in the northeastern Greenland Sea and Fram Strait, seems counterintuitive since these regions receive extra surface fresh-water in the Fram experiment. The explanation for the seeming inconsistency lies in the pattern itself, which resembles the Western Spitsbergen Current transporting North Atlantic water into the Arctic. The salinity increase of aforementioned regions is thus due to the strengthening of the MOC. Compared to the upper-level pattern, the salinity anomaly in the lower layers is uniformly positive over the entire Arctic (Fig. 12b). This can be caused by a weakened deep overflow in the Fram experiment which produces a weaker export of the relatively salty deep water from the Arctic. The increase in salinity in the subpolar lower-level water can be due either to the southward propagation of positive salinity anomaly signal in higher latitudes, or vertical penetration of the upper-level salinity increase through the deep convection in the Labrador Sea. One related question in Arctic climate research is whether the observed ice thinning in

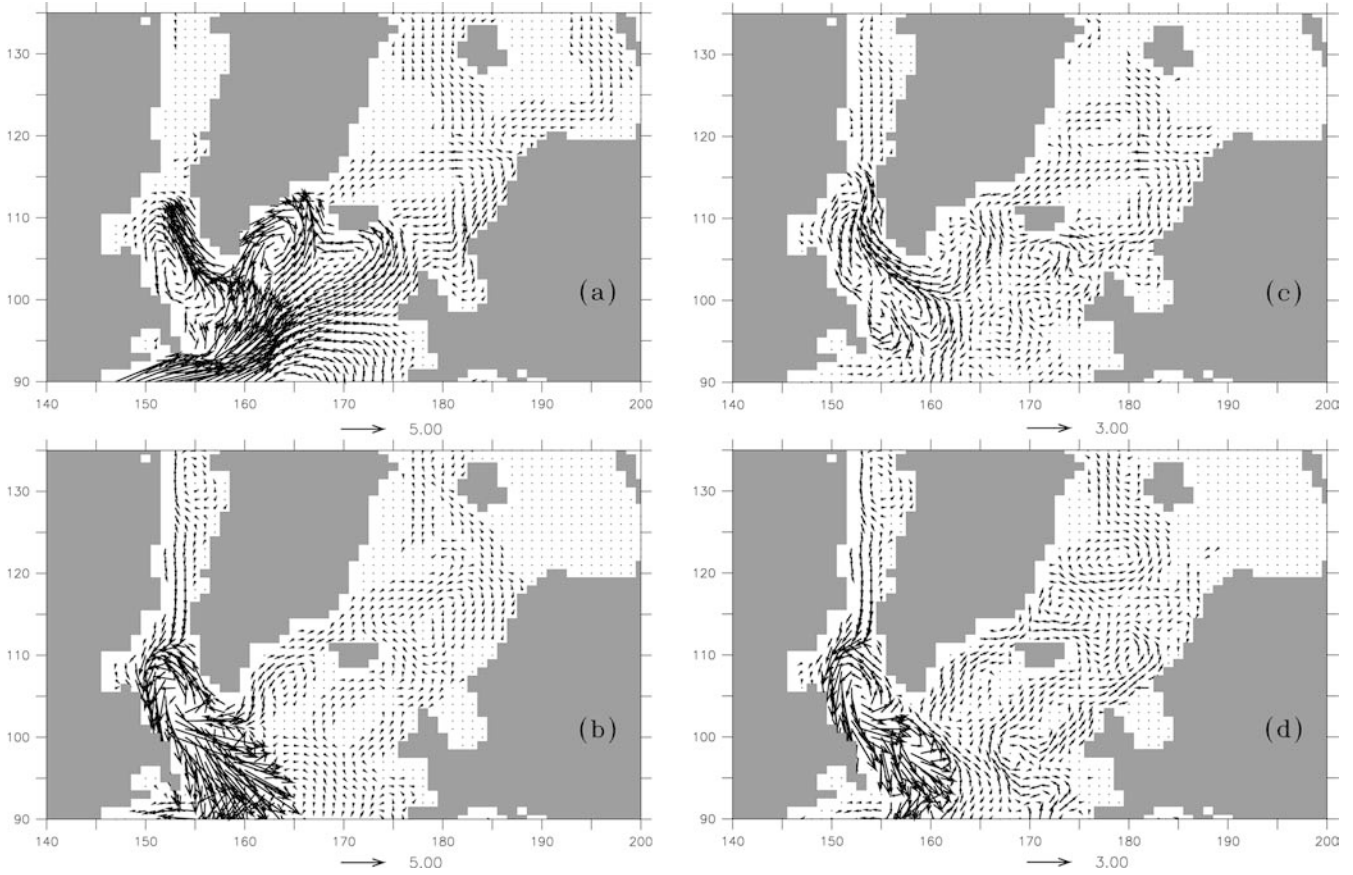


Fig. 10 Along isopycnal surface volume transports (unit: Sv) in the Fram experiment vertically integrated over layers **a** 1–12 and **b** 13–16 respectively. Differences between the Fram and Baffin experi-

ments (Fram – Baffin) of the transport are shown in **c** (over layers 1–12) and **d** (for layers 13–16)

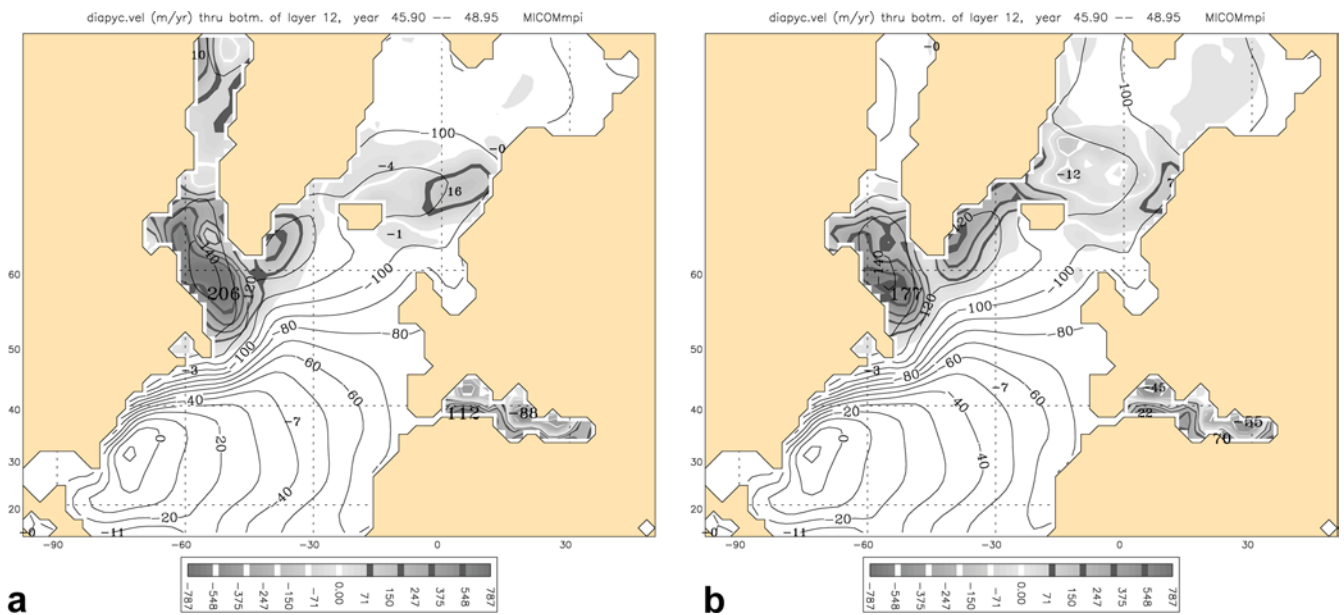


Fig. 11a, b Diapycnal mass transport (unit: m/year) across the upper interface of $\sigma_2 = 36.95$ (gray shading). Numbers represent the same variable spatially integrated (units: $10 \times Sv$). The thin lines

represent mean sea surface height (units: cm). **a** Fram experiment, **b** Baffin experiment

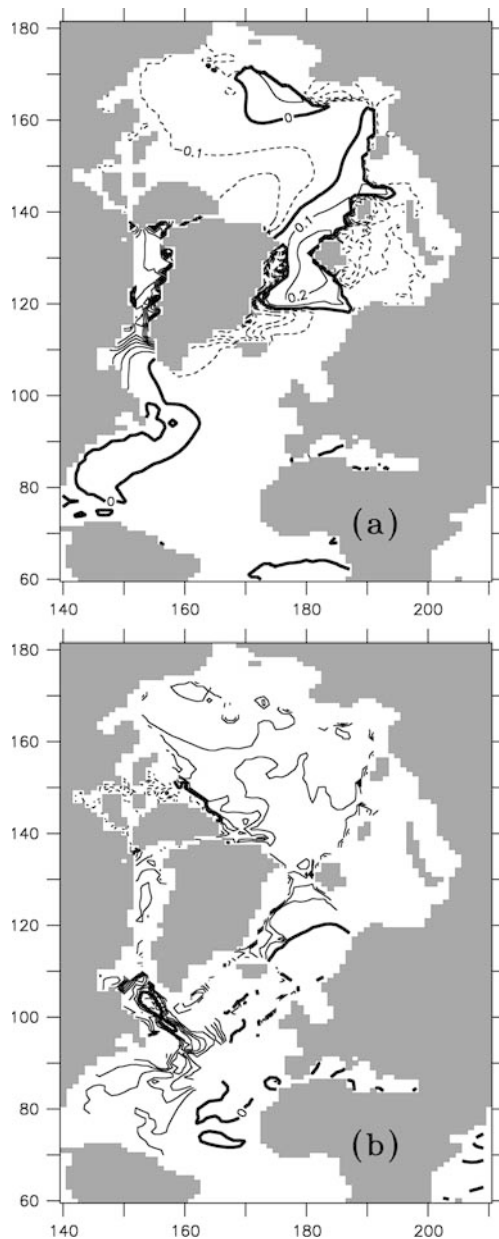


Fig. 12 Salinity difference between the Fram and Baffin experiment (Fram minus Baffin) averaged over **a** layers 1–12 and **b** layers 13–16, respectively. Contour interval in **a** and **b** is 0.1 psu and 0.03 psu

recent decades (Rothrock et al. 1999) is caused by changing atmospheric conditions such as warming or changes in the wind field (Rigor et al. 2001), or else by changing oceanic heat and fresh-water import into the Arctic (Holland et al. 2001). In our simulations, corresponding to a 15% increase in the MOC, thinning of sea ice in the central Arctic is 1–2% of its long term mean (not shown). Thinning of sea ice in the Nordic Seas is more significant in terms of percentage to its climatological values, and the absolute amplitude is on the order of tens of centimeters. Given the pure thermodynamic nature of the ice model used in this study and fixed

surface atmospheric conditions, this thinning is due entirely to the warming of the upper ocean caused by a stronger overturning.

4 Summary

As a first step towards understanding the advective contribution of surface fresh-water flux to the MOC and subsequently on the global climate involving a coupled atmosphere–ocean–ice model, in this study we have examined the quasi-equilibrium states of the MOC in the ocean-only runs driven by climatological surface forcing conditions.

The maximum annual mean Atlantic overturning stream function in the model is sensitive to the location of surface fresh-water transport perturbations. When the globally averaged net surface fresh-water flux are held constant, an Arctic ice related fresh-water transport of 0.1 Sv entering the Nordic Seas reduces the maximum overturning in the Atlantic by 1 to 2 Sv. The MOC is further reduced by 3 to 5 Sv when the fresh-water transport anomaly is instead shifted to the southern Baffin Bay area. These results thus suggest that between the Labrador Sea Water and the overflows across the Greenland–Scotland Ridge, the former plays a determining role in governing the MOC and its overall sensitivity in the simulation. We found that such a dominance is not due solely to an undersimulation of the overflows simulated in the model, since examinations of the transport amplitudes of the overflow and its θ/S evolution along the circulation pathways indicate that the simulations have captured some of the basic characters of observations.

These conclusions are further supported by surface injected tracer simulations which show that the subpolar and mid-latitude deep Atlantic is ventilated by water originated in the surface layer of the Greenland–Norwegian and Labrador Seas. There are distinctive pathways associated with either water mass. However, although the separation of the two water masses is exhibited to some degree in the model, it is probably not as strong as in nature.

The 3 to 5 Sv difference in the magnitude of the MOC is comparable to multi-decadal MOC variability observed in coupled ocean–atmosphere models (e.g., Delworth et al. 1993; Cheng et al. 2004). The fresh-water transport perturbation used to drive this change is on the order of the observed long-term mean ice flux through the Fram Strait in present day climate. Although the interannual variability of the ice flux in current climate is only 10–15% of its long-term mean, climate models have predicted massive change of the North Atlantic fresh-water flux under global warming scenarios. It is these larger climate shifts that relate to our amplitude of fresh-water anomaly.

On the interactions between the overflow and the Labrador Sea Water, a see-saw relationship is found: when the Labrador Sea water formation strengthens, the

overflow transport weakens even though the surface forcing conditions are held constant in its formation region. Such a response in the overflow is hence more likely controlled by ocean internal processes which we suspect are related to determining the ocean internal stratification.

It is well known that the MOC in the ocean fluctuates on multiple time scales, the fastest of which is decadal to multi-decadal and controlled by basin-scale advective and planetary wave processes in the mid- to high latitudes (Bjerknes 1964; Latif and Barnett 1996; Sutton and Allen 1997; Saravanan and McWilliams 1998; Grötzner et al. 1998). In addition to ocean internal dynamics (e.g., Winton and Sarachik 1993; Weaver and Sarachik 1991), variability of the MOC can also be excited by low-frequency variations in the surface forcing conditions. What drives fluctuations in the air-sea exchange fluxes, moreover, whether it requires participation of both the atmosphere, the ocean, and the sea ice, is not addressed in this study. These matters need to be investigated in a fully coupled ocean-atmosphere-sea ice model and are subjects of our ongoing research.

Acknowledgements We acknowledge the valuable input from Drs. Jonathan Lilly, David Bailey, and Jerome Cuny during the course of this study. This research is supported by a grant from the Vetlesen Foundation to the University of Washington.

References

- Arfken G (1970) *Mathematical methods for physicists* 2nd edn. Academic Press, San Diego pp 815
- Belkin IM, Levitus S, Antonov J, Malmberg SA (1998) "Great Salinity Anomalies" in the North Atlantic. *Prog Oceanogr* 41: 1–68
- Bjerknes J (1964) Atlantic air-sea interaction. *Adv Geophys* 20: 1–82
- Bleck R, Boudra D (1986) Wind-driven spin-up in eddy-resolving ocean models formulated in isopycnal and isobaric coordinates. *J Geophys Res* 91: 7611–7621
- Bleck R, Hanson H, Hu D, Kraus E (1989) Mixed layer/thermocline interaction in a three-dimensional isopycnal model. *J Phys Oceanogr* 19: 1417–1439
- Cheng W, Bleck R, Rooth C (2004) Multi-decadal thermohaline variability in an ocean-atmosphere general circulation model. *Clim Dyn* (in press)
- Delworth TL, Dixon KW (2000) Implications of the recent trend in the Arctic/North Atlantic Oscillation for the North Atlantic thermohaline circulation. *J Clim* 13: 3721–3727
- Delworth TL, Manabe S, Stouffer RJ (1993) Interdecadal variations of the thermohaline circulation in a coupled ocean-atmosphere model. *J Clim* 6: 1993–2011
- Deser C, Walsh JE, Timlin MS (2000) Arctic sea ice variability in the context of recent atmospheric circulation trends. *J Clim* 13: 617–633
- Dickson R, Lazier J, Meincke J, Rhines P, Swift J (1996) Long-term coordinated changes in the convective activity of the North Atlantic. *Prog Oceanogr* 38: 241–295
- Dickson RR, Brown J (1994) The production of North Atlantic Deep Water: sources rates and pathways. *J Geophys Res* 99: 12,319–12,341
- Dickson RR, Osborn TJ, Hurrell JW, Meincke J, Blindheim J, Adlandsvik B, Vinje T, Alekseev G, Maslowski W (2000) The Arctic Ocean response to the North Atlantic Oscillation. *J Clim* 13: 2671–2696
- Döscher R, Redler R (1997) The relative importance of northern overflow and subpolar deep convection for the North Atlantic thermohaline circulation. *J Phys Oceanogr* 27: 1894–1902
- Girton JB, Sanford TB (2001) Synoptic sections of the Denmark strait overflow. *Geophys Res Lett* 28: 1619–1622
- Goosse H, Fichofet T, Campin JM (1997) The effects of the water flow through the Canadian Archipelago in a global ice-ocean model. *Geophys Res Lett* 24: 1507–1510
- Griffies SM, Pacanowski RC, Hallberg RW (2000) Spurious diapycnal mixing associated with advection in a z-coordinate ocean model. *Mon Weather Rev* 128: 538–564
- Grötzner AM, Latif M, Barnett TP (1998) A decadal climate cycle in the North Atlantic Ocean as simulated by the ECHO coupled GCM. *J Clim* 11: 831–847
- Hansen B, Turrell WR, Østerhus S (2001) Decreasing overflow from the Nordic Seas into the Atlantic Ocean through the Faroe Bank channel since 1950. *Nature* 411: 927–930
- Holland MM, Bitz CM, Eby M, Weaver AJ (2001) The role of ice-ocean interactions in the variability of the North Atlantic thermohaline circulation. *J Clim* 14: 656–675
- Hurrell JW (1995) Decadal trends in the North Atlantic Oscillation: regional temperatures and precipitation. *Science* 269: 676–679
- Kraus E, Turner J (1967) A one-dimensional model of the seasonal thermocline. Part 2. The general theory and its consequences. *Tellus* 19: 98–106
- Kwok R, Rothrock D (1999) Variability of Fram Strait ice flux and North Atlantic Oscillation. *J Geophys Res* 104: 5177–5189
- Latif M, Barnett TP (1996) Decadal climate variability over the North Pacific and North America: dynamics and predictability. *J Clim* 9: 2407–2423
- Levitus S (1994) *World ocean Atlas 1994 CD-Rom sets*. National Oceanographic Data Center Informal Rep 13
- MacDougall TJ, Dewar WK (1998) Vertical mixing and cabbeling in layered models. *J Phys Oceanogr* 28: 1458–1480
- Manabe S, Stouffer RJ (1995) Simulation of abrupt climate change induced by freshwater input to the North Atlantic Ocean. *Nature* 378: 165–167
- Marotzke J, Scott JR (1999) Convective mixing and the thermohaline circulation. *J Phys Oceanogr* 29: 2962–2970
- Mauritzen C (1996) Production of dense overflow waters feeding the North Atlantic across the Greenland-Scotland Ridge Part 2: an inverse model. *Deep Sea Res* 6: 807–835
- Mauritzen C, Häkkinen S (1999) On the relationship between densewater formation and the "Meridional Overturning Cell" in the North Atlantic Ocean. *Deep Sea Res I* 46: 877–894
- McCartney MS (1992) Recirculating components to the deep boundary current of the northern North Atlantic. *Prog Oceanogr* 29: 283–383
- McCartney MS, Talley LD (1984) Warm-to-cold water conversion in the Northern North Atlantic Ocean. *J Phys Oceanogr* 14: 922–935
- Perry G, Duffy P, Miller N (1996) An extended data set of river discharges for validation of general circulation models. *J Geophys Res* 101: 21,339–21,349
- Rigor IG, Wallace J, Colony R (2002) Response of sea ice to the Arctic Oscillation. *J Clim* 15: 2648–2668
- Rothrock DA, Yu Y, Maykut GA (1999) Thinning of the Arctic sea-ice cover. *Geophys Res Lett* 26: 3469–3472
- Saravanan R, McWilliams JC (1998) Advective ocean-atmosphere interaction: an analytical stochastic model with implications for decadal variability. *J Clim* 11: 165–188
- Schmitz WJ (1995) On the inter-basin scale thermohaline circulation. *Rev Geophys* 33: 151–173
- Semtner AJ (1976) Model for thermodynamic growth of sea ice in numerical investigations of climate. *J Phys Oceanogr* 6: 379–389
- Send U, Marshall J (1995) Integral effects of deep convection. *J Phys Oceanogr* 25: 855–872
- Spall M, Pickart RS (2001) Where does dense water sink? A subpolar gyre example. *J Phys Oceanogr* 31: 810–826
- Speer K, Tziperman E (1992) Rates of water mass formation in the North Atlantic Ocean. *J Phys Oceanogr* 22: 93–104

- Sutton RT, Allen MR (1997) Decadal predictability of North Atlantic sea surface temperature and climate. *Nature* 388: 563–567
- Thompson DWJ, Wallace JM (2000) Annular modes in the extratropical circulation. Part I. Month-to month variability. *J Clim* 13: 1000–1016
- Veronis G (1975) The role of models in tracer studies. Numerical models of ocean circulation. National Academy of Science, pp 133–146
- Washington L (1976) On the North Atlantic circulation. *Johns Hopkins Oceanogr Stud* 6: 110
- Weaver AJ, Sarachik ES (1991) Evidence for decadal variability in an ocean general circulation model: an advective mechanism. *Atmos Ocean* 29: 197–231
- Winton M, Sarachik ES (1993) Thermohaline oscillations induced by strong steady salinity forcing of ocean general circulation models. *J Phys Oceanogr* 23: 1389–1410
- Zhang J, Rothrock D, Steele M (2000) Recent changes in Arctic sea ice: the interplay between ice dynamics and thermodynamics. *J Clim* 13: 3099–3114